

Effects of Surface and Plate-Gap Discharges on Panel-Aging Characteristics in Alternating-Current Plasma Display Panel

Choon-Sang Park and Heung-Sik Tae*

School of Electronics Engineering, College of IT Engineering, Kyungpook National University, Daegu 702-701, Republic of Korea

Received October 21, 2011; accepted April 28, 2012; published online September 20, 2012

In this study, we investigate the changes in surface morphology of the MgO layer on both the bus and indium tin oxide (ITO) electrodes in an alternating-current (AC) plasma display panel (PDP) under the surface and plate-gap discharges during the panel-aging process. It is found that the use of the surface discharge mixed with the plate-gap discharge during the panel-aging process contributes to obtaining uniform MgO surface morphologies for both bus and ITO electrodes within a fast panel-aging process time. © 2012 The Japan Society of Applied Physics

1. Introduction

Recently, to lower the panel fabrication cost, the plasma display panel (PDP) industry has focused on reducing the panel-aging process time in AC-PDPs, particularly for full-high definition (FHD) PDPs with very small discharge cells. The initial surface states of the MgO layer after deposition by the ion-plating method are very nonuniform.¹⁻¹¹ Accordingly, the panel-aging process is required to obtain uniform MgO surface morphologies on both the bus and indium tin oxide (ITO) electrodes for stable discharge. Therefore, the surface state of the MgO surface in the front panel after the panel-aging process is important for producing stable reset and address discharges in PDP cells, as the discharge characteristics can vary depending on the state of the MgO surface.¹²⁻¹⁵ Moreover, our previous experiments showed that the variations in the surface states of the MgO layer with respect to the ion bombardments during the panel-aging process were very important for determining the formative and statistical address delay times (T_f and T_s , respectively).¹⁵ These parameters are significant factors for determining a stable driving margin for a PDP. One of the methods employed to reduce the panel-aging process time is simply to use a higher sustain voltage during the panel-aging process. However, our previous experimental results also showed that the use of a higher sustain voltage during the panel-aging process resulted in unstable discharge owing to the nonuniform surface morphologies of the MgO thin film on the bus and ITO electrodes caused by the occurrence of a self-erasing discharge.¹⁶ Several efforts to reduce panel-aging process time have been reported, such as the use of driving waveforms, plasma pretreatment, and a vacuum sealing process.¹⁷⁻¹⁹ However, the correlations between the surface and plate-gap discharge mode and the discharge and surface characteristics of the MgO layer in the display cell during the panel-aging process are still not well known.

Accordingly, in this study, we examine the changes in the surface morphology of the MgO layer on the bus and ITO electrodes under the surface and plate-gap discharges during the panel-aging process. The used test panels are a 50 in. FHD AC-PDP with a He (35%)–Xe (11%)–Ne gas composition and box-type barrier under a pressure of 430 Torr.

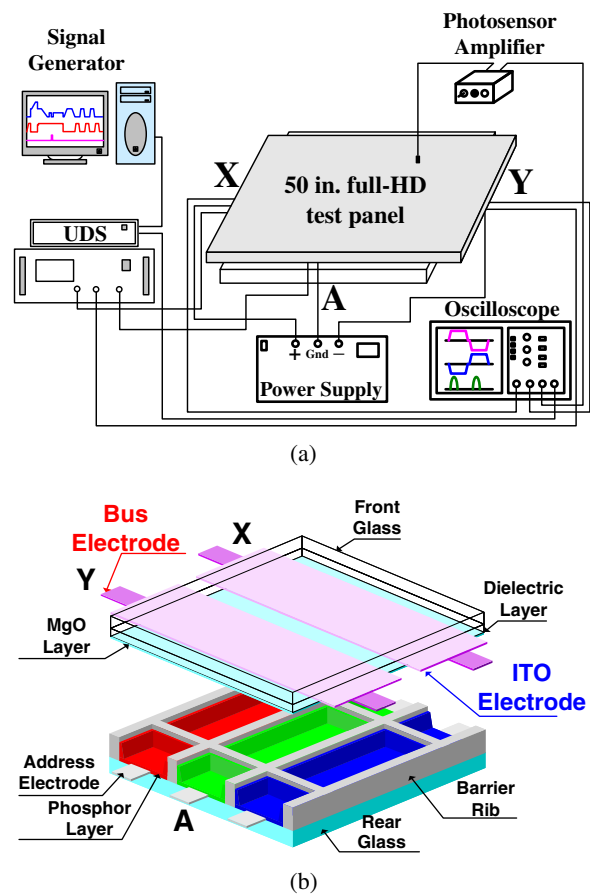


Fig. 1. (Color online) Schematic diagram of (a) experimental setup employed in this research and (b) single pixel structure in 50 in. FHD AC-PDP.

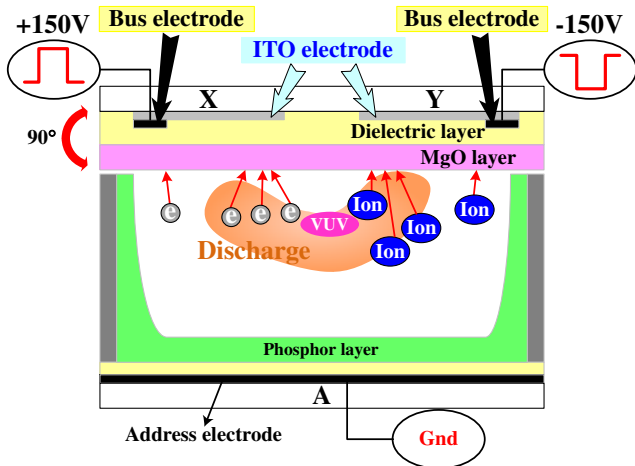
2. Experimental Methods

Figure 1(a) shows the optical measurement system and 50 in. FHD test panel with three electrodes used in this experiment, where X is the sustain electrode, Y is the scan electrode, and A is the address electrode. A signal generator and photo sensor amplifier (Hamamatsu C6386) were used to measure the IR emission and address delay time, respectively. Figure 1(b) shows a schematic diagram of a single pixel from the 50 in. FHD AC-PDP panel employed in this experiment. The ITO electrode had a low conductivity, whereas the bus electrode made from silver had a high conductivity. The gap between the two ITO

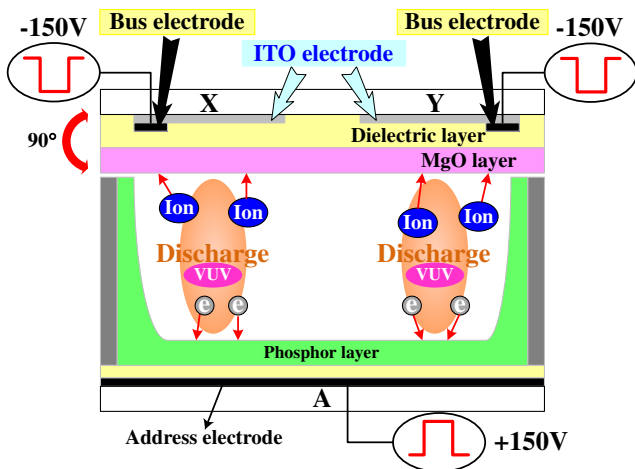
*E-mail address: hstae@ee.knu.ac.kr

Table I. Specifications of 50 in. FHD AC-PDP test panels employed in this research.

Front panel		Rear panel	
ITO width (μm)	210	Barrier rib width (μm)	50
ITO gap (μm)	70	Barrier rib height (μm)	120
Bus width (μm)	70	Address width (μm)	85
Cell pitch (μm^2)	192 \times 576		
Gas chemistry	Ne–Xe (11%)–He (35%)		
Gas pressure (Torr)	430		
Barrier rib type	Closed rib		



(a)



(b)

Fig. 2. (Color online) Comparison of (a) surface and (b) plate-gap discharges during panel-aging process in ac-PDP cell.

electrodes was short, whereas the gap between the bus electrodes was long. The detailed panel specifications are listed in Table I. The gas composition was He (35%)–Xe (11%)–Ne under a pressure of 430 Torr.

Figures 2(a) and 2(b) show schematic diagrams for surface and plate-gap discharges during the panel-aging process in an ac-PDP cell. In Fig. 2(a), the surface discharge was produced by applying +150 and –150 V to the X and Y electrodes of the test panel, respectively, whereas in Fig. 2(b), the plate-gap discharge was produced by applying –150, –150, and +150 V to the X, Y, and A electrodes of

	SEM images		Panel-aging process time
	On bus electrode	On ITO electrode	
(a) Surface discharge			12 h
(b) Plate-gap discharge			8 h
(c) Surface discharge → Plate-gap discharge			4 h
(d) Plate-gap discharge → Surface discharge			4 h

Fig. 3. (Color online) Comparison of SEM images of MgO surface changes on bus and ITO electrodes after panel-aging process measured from 50 in. FHD panels and panel-aging process time detected by human eyes under various discharge modes such as (a) surface, (b) plate-gap, (c) plate-gap discharge after surface discharge, and (d) surface discharge after plate-gap discharge.

the test panel, respectively. The duty ratio and frequency for the sustain period were 40% and 25 kHz, respectively. As shown in Fig. 2, the gap between the two ITO electrodes was short, whereas the gaps between the bus electrodes and between the sustain (ITO) and address electrodes were longer. The surface discharge gaps between the ITO electrodes and between the bus electrodes in Fig. 2(a) are 70 and 330 μm , respectively, whereas the plate-gap discharge between the sustain (ITO) and address electrodes in Fig. 2(b) is 135 μm . Therefore, at the same voltage level, in the case of using only the surface discharge (conventional), strong surface discharge was confined within the ITO electrode, whereas in the case of using only the plate-gap discharge, weak plate-gap discharges were produced over the whole regions of both the bus and ITO electrodes.

3. Results and Discussion

3.1 Change in surface characteristics of MgO layer with panel-aging process time

Figure 3 shows scanning electron microscopy (SEM) images of the MgO surface on the bus and ITO electrodes after the panel-aging process time detected by human eyes under various discharge modes such as (a) surface, (b) plate-gap, (c) plate-gap discharge after surface discharge, and (d) surface discharge after plate-gap discharge in the 50 in. FHD test panels. Table II shows the roughness of the MgO surface on the bus and ITO electrodes determined by atomic-force microscopy (AFM) analysis after the panel-aging process under various discharge modes. In this case, the panel-aging process time was chosen simply by human eyes under various discharge modes in Fig. 3. During the panel-aging process, the discharge states were observed by the human eyes until the unstable discharge was eliminated in the entire region of the 50 in. FHD test panels. In Fig. 3(a),

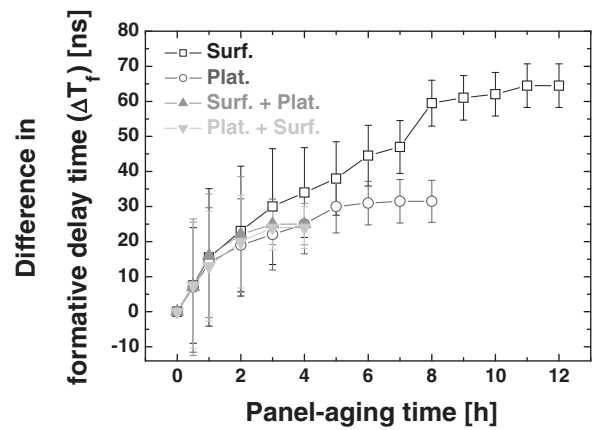
Table II. Comparison of roughness of MgO surface changes on bus and ITO electrodes based on AFM analysis after panel-aging process measured from 50 in. FHD panels under various discharge modes such as surface, plate-gap, plate-gap discharge after surface discharge, and surface discharge after plate-gap discharge.

	Roughness (rms, Å)	
	On bus electrode	On ITO electrode
Surface discharge	75.8	142.6
Plate-gap discharge	119.8	102.4
Surface discharge → plate-gap discharge	54.2	58.7
Plate-gap discharge → surface discharge	52.3	55.1

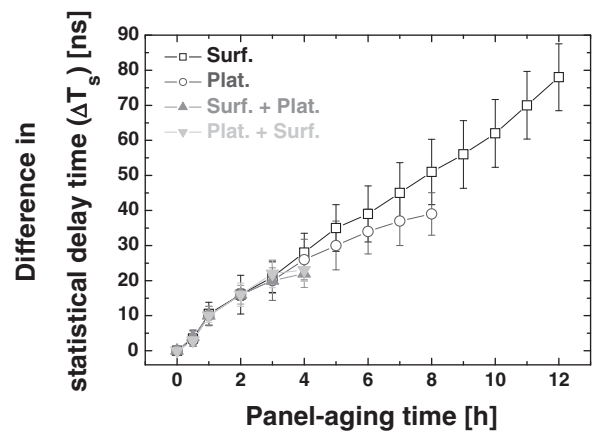
the panel-aging process was carried out by using only the surface discharge shown in Fig. 2(a). As shown in Fig. 3(a) and Table II, the MgO surface morphology and roughness on the ITO electrode were observed to be larger and higher than those on the bus electrode, respectively. This also means that pyramidal or cubic morphology of the grains on the MgO surface on the ITO electrode was eliminated.¹⁵⁾ The total panel-aging process time was about 12 h. In Fig. 3(b), the panel-aging process was carried out by using only the plate-gap discharge shown in Fig. 2(b). As shown in Fig. 3(b) and Table II, the MgO surface morphologies and roughnesses for both bus and ITO electrodes were observed to be almost the same and the total panel-aging process time was about 8 h. We have reported that continuous ion bombardment on the MgO thin film causes the surface morphology and roughness of the MgO thin film to increase.^{15,20–24)} The surface morphologies and roughnesses in the case of using only the surface discharge of Fig. 3(a) and Table II meant that the MgO surface on the ITO electrode was struck by many more ions than that on the bus electrode, implying that the strong discharge did not spread towards the bus electrode owing to the confined strong surface discharge within the ITO electrode. On the other hand, in the case of using only the plate-gap discharge, the MgO surfaces on both the bus and ITO electrodes were struck severely, implying that weak plate-gap discharges were produced over the whole region of both the bus and ITO electrodes. Furthermore, the uniform MgO surface on both the bus and ITO electrodes was able to produce a stable discharge.

As shown in Figs. 3(c) and 3(d), the panel-aging process was carried out by using the surface discharge mixed with the plate-gap discharge. The conditions for the surface discharge mixed with the plate-gap discharge were as follows: the testing times for the surface and plate-gap discharges were both 2 h, and the interval time between the surface and plate-gap discharges was about 1 min. In Fig. 3(c), the plate-gap discharge was used after the surface discharge during the panel-aging process, whereas in Fig. 3(d), the surface discharge was used after the plate-gap discharge during the panel-aging process. In these cases, the MgO surface morphologies and roughnesses for both bus and ITO electrodes were observed to be almost the same. In addition, the total panel-aging process times were all about 4 h.

The SEM images of Fig. 3 and the roughnesses of Table II illustrate that the surface discharge mixed with the



(a)



(b)

Fig. 4. Comparison of (a) formative (ΔT_f) and (b) statistical (ΔT_s) address delay time differences during panel-aging time measured from 50 in. FHD panels under various discharge modes such as surface (Surf.), plate-gap (Plat.), plate-gap discharge after surface discharge (Surf. + Plat.), and surface discharge after plate-gap discharge (Plat. + Surf.).

plate-gap discharge contributes to shortening the panel-aging process time, implying that the uniform MgO surface on both bus and ITO electrodes for stable discharge was able to be obtained within a fast process time in the cases of adopting the surface discharge mixed with the plate-gap discharge during the panel-aging process.

3.2 Change in address discharge characteristics during panel-aging process

Figure 4 shows the changes in (a) the formative address delay time ($= \Delta T_f$) and (b) the statistical address delay time ($= \Delta T_s$) during the panel-aging process under various discharge modes such as surface, plate-gap, plate-gap discharge after surface discharge, and surface discharge after plate-gap discharge in the 50 in. FHD test panels. As shown in Fig. 4(a), in the cases of both the surface and plate-gap plasma discharges, the formative address delay times were observed to be increased continuously during the panel-aging process. The formative address delay times for the surface and plate-gap plasma discharge cases were stabilized in about 11 and 6 h, respectively. However, in both cases of the surface discharge mixed with the plate-gap discharge, the formative address delay times were stabilized in a short period of time (about 3 h) after the aging process started.

As shown in Fig. 4(b), in both cases of the surface and plate-gap plasma discharges, the statistical address delay times were observed to be increased quickly during the panel-aging process. However, in both cases of the surface discharge mixed with the plate-gap discharge, the statistical address delay times were observed to be increased gradually during the panel-aging process. In conclusion, the surface discharge mixed with the plate-gap discharge can equalize the MgO surface on both bus and ITO electrodes easily and quickly, and as such can shorten the aging process time by quickly stabilizing the discharge characteristics such as formative address delay time and statistical address delay time, which are requisite for stable discharge.

4. Conclusions

In this work, the surface discharge mixed with the plate-gap discharge modes were adopted to reduce the panel-aging process time. For both cases of the surface discharge mixed with the plate-gap discharge in the 50 in. FHD ac-PDP, the changes in the discharge characteristics during the panel-aging process, such as the formative address delay time and statistical address delay time, were examined. Our experimental results confirmed that the surface discharge mixed with the plate-gap discharge was able to make the MgO surface morphologies on both the bus and ITO electrodes uniform within a short aging process time, thereby resulting in stable panel-aging discharge characteristics in PDP panels with very small discharge cells.

Acknowledgements

This work was supported in part by the Basic Science Research Program through the National Research Foundation of Korea (NRF) funded by the Ministry of Education, Science and Technology (2012-0004506) and in part by Brain Korea 21 (BK21).

- 1) K. C. Choi, H.-J. Kim, and B. J. Shin: *IEEE Trans. Electron Devices* **51** (2004) 1241.
- 2) B. K. Song, Y. J. Lee, C. H. Yi, H. K. Hwang, and G. Y. Yeom: *Jpn. J. Appl. Phys.* **42** (2003) L74.
- 3) K. Refson, R. A. Wogelius, D. G. Fraser, M. C. Payne, M. H. Lee, and V. Milman: *Phys. Rev. B* **52** (1995) 10823.
- 4) M. S. Park, D. H. Park, B. H. Kim, B. G. Ryu, S. T. Kim, G.-W. Seo, D.-Y. Kim, S.-T. Park, and J.-B. Kim: *Dig. Int. Meet. Information Display*, 2006, p. 126.
- 5) J. K. Kim, K. S. Moon, and K. W. Whang: *J. Vac. Sci. Technol. B* **19** (2001) 687.
- 6) K.-H. Park, M.-S. Ko, S.-H. Yoon, and Y.-S. Kim: *Dig. Int. Meet. Information Display*, 2007, p. 216.
- 7) P. Pleshko: *IEEE Trans. Electron Devices* **28** (1981) 654.
- 8) C.-H. Park, Y.-K. Kim, B.-E. Park, W.-G. Lee, and J.-S. Cho: *Mater. Sci. Eng. B* **60** (1999) 149.
- 9) M. O. Aboelfotoh and O. Sahni: *IEEE Trans. Electron Devices* **28** (1981) 645.
- 10) M. Noh, Y. Yi, and K. Jeong: *J. Korean Phys. Soc.* **42** (2003) 631.
- 11) K. Uchida, G. Uchida, T. Kurauchi, T. Terasawa, H. Kajiyama, and T. Shinoda: *Dig. Int. Display Workshops*, 2006, p. 347.
- 12) C.-S. Park and H.-S. Tae: *Appl. Phys. Lett.* **96** (2010) 043504.
- 13) C.-S. Park, H.-S. Tae, and S.-I. Chien: *Appl. Phys. Lett.* **99** (2011) 083503.
- 14) C.-S. Park, S.-Y. Kim, E.-Y. Jung, and H.-S. Tae: *Jpn. J. Appl. Phys.* **50** (2011) 070210.
- 15) C.-S. Park, H.-S. Tae, E.-Y. Jung, J. H. Seo, and B. J. Shin: *IEEE Trans. Plasma Sci.* **38** (2010) 2439.
- 16) C.-S. Park, H.-S. Tae, E.-Y. Jung, and J.-C. Ahn: *Thin Solid Films* **518** (2010) 6153.
- 17) C.-S. Park, J. H. Kim, and H.-S. Tae: *Dig. Int. Conf. Microelectronics and Plasma Technology*, 2011, p. 115.
- 18) C.-S. Park, S.-K. Jang, H.-S. Tae, and E.-Y. Jung: *Mol. Cryst. Liq. Cryst.* **551** (2011) 95.
- 19) K. Uchida, G. Uchida, T. Yano, H. Kajiyama, and T. Shinoda: *Dig. Int. Display Workshops*, 2008, p. 1899.
- 20) C.-S. Park, S.-K. Jang, H.-S. Tae, E.-Y. Jung, and J.-C. Ahn: *J. Soc. Inf. Disp.* **17** (2009) 977.
- 21) C.-S. Park, S.-Y. Kim, J. H. Kim, and H.-S. Tae: *Mol. Cryst. Liq. Cryst.* **551** (2011) 104.
- 22) C.-S. Park and H.-S. Tae: *Appl. Opt.* **48** (2009) F76.
- 23) S.-K. Kwon, J.-H. Kim, S.-K. Moon, J.-K. Choi, Y.-I. Jang, K.-H. Park, and S.-S. Han: *SID Int. Symp. Dig. Tech. Pap.* **40** (2009) 359.
- 24) C.-S. Park, J. H. Kim, S.-K. Jang, H.-S. Tae, and E.-Y. Jung: *J. Soc. Inf. Disp.* **18** (2010) 606.